Supporting Information

Effective Aperture Tuning of a Zeolitic-Imidazole Framework CdIF-1 by Controlled Thermal Amorphization

Sunghwan Park[a] and Hae-Kwon Jeong*[ab]

[a] Artie McFerrin Department of Chemical Engineering and [b] Department of Materials Science and Engineering, Texas A&M University, 3122 TAMU, College Station, TX 77843-3122, United States

** Corresponding author:*

H.-K. Jeong (E-mail address: hjeong7@tamu.edu, Phone: +1-979-862-4850, Fax: +1-979-845-6446)

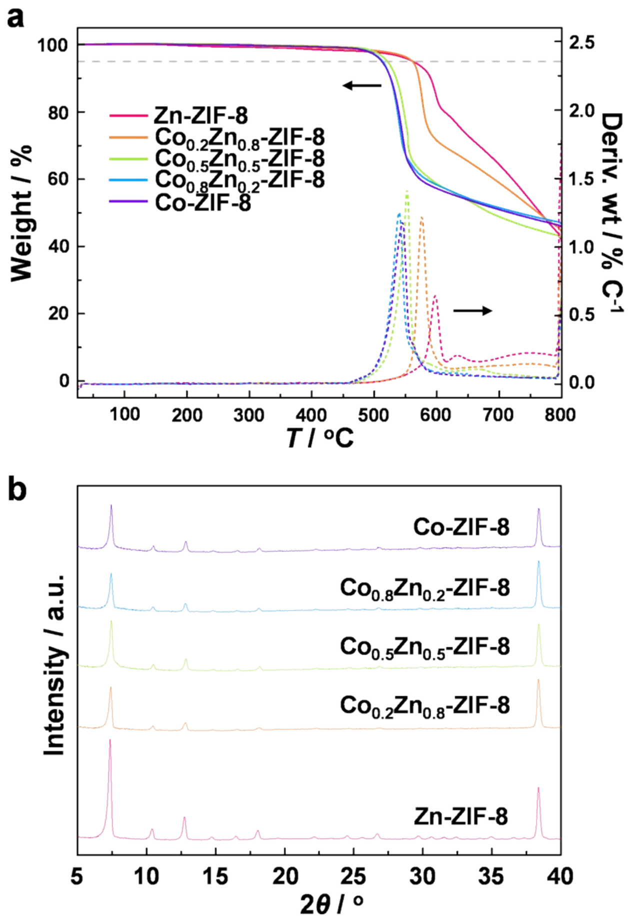

Figure S1. (a) TGA thermogram of ZIF-8, ZIF-67, and CoZn-ZIF-8. (b) XRD patterns of ZIF-8, ZIF-67, and CoZn-ZIF-8 heat-treated at T_d (95 wt%) determined in (a).

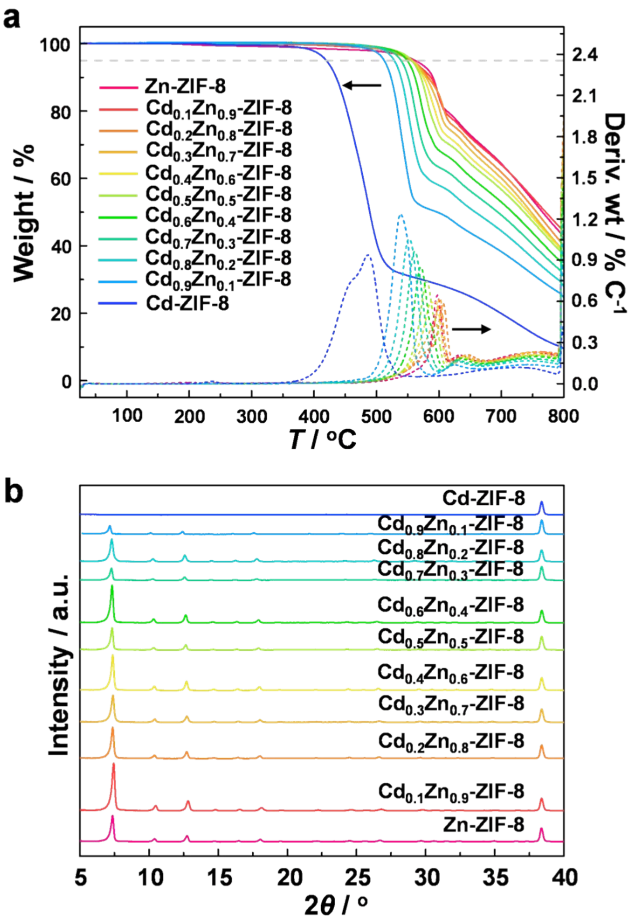

Figure S2. (a) TGA thermogram of ZIF-8, CdIF-1, and CdZn-ZIF-8. (b) XRD patterns of ZIF-8, CdIF-1, and CdZn-ZIF-8 heat-treated at T_d (95 wt%) determined in (a).

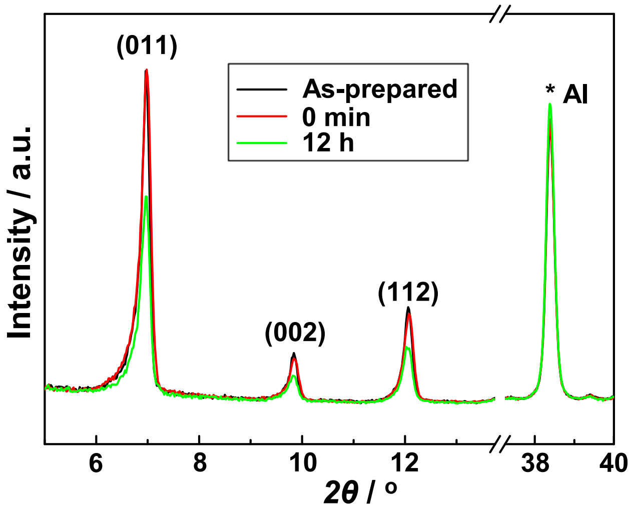

Figure S3. XRD patterns of CdIF-1 heat-treated at 220 °C with different soaking times.

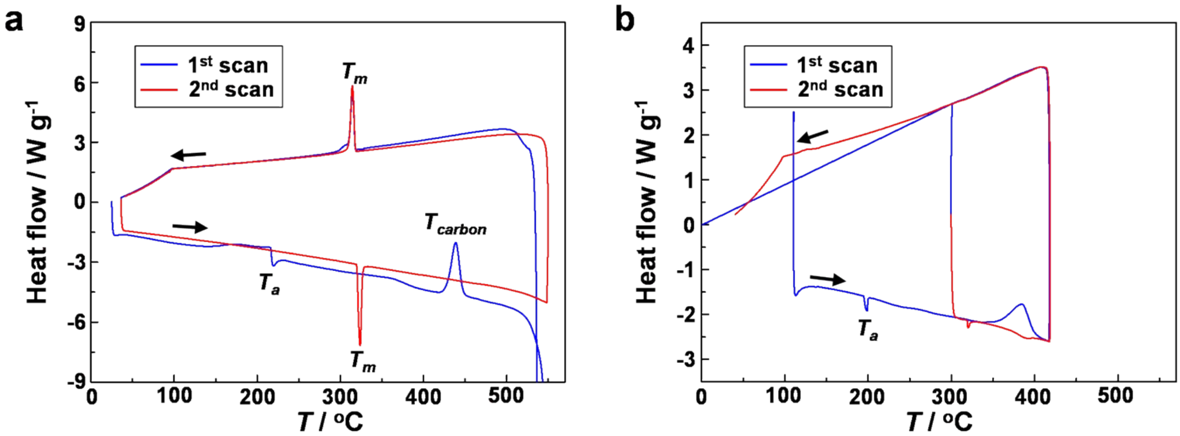

Figure S4. DSC curves of CdIF-1 with the final temperature of (a) 550 °C and (b) 420 °C.

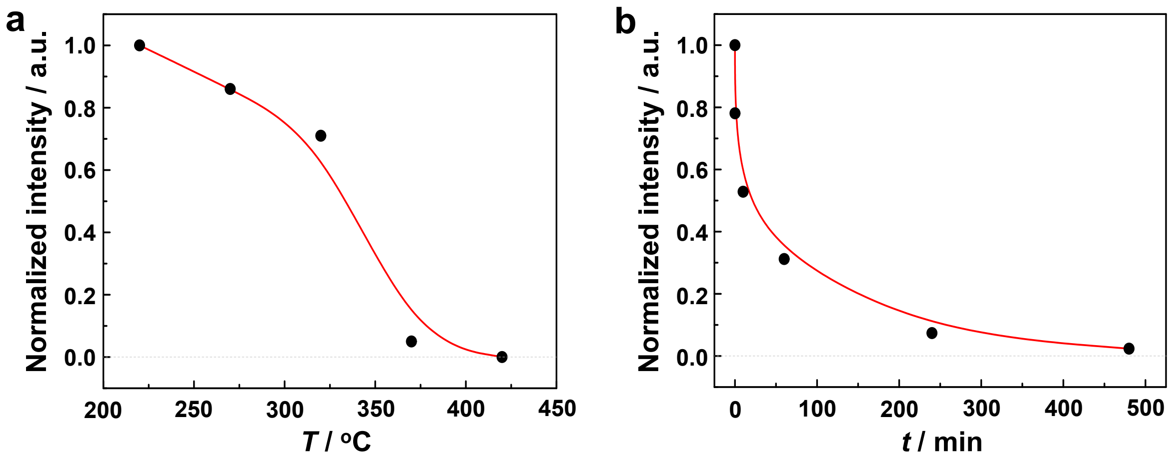

Figure S5. Normalized (110) peak intensity of XRD patterns of CdIF-1 with (a) different heating temperatures and (b) different soaking times at 320 ºC.

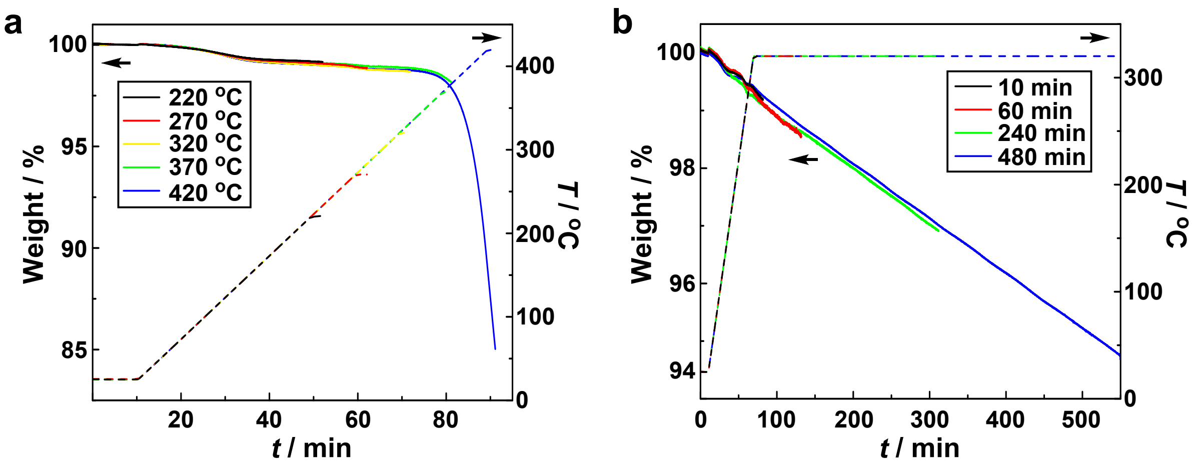

Figure S6. TGA thermogram of CdIF-1 with (a) different heating temperatures and (b) different soaking times at 320 °C.

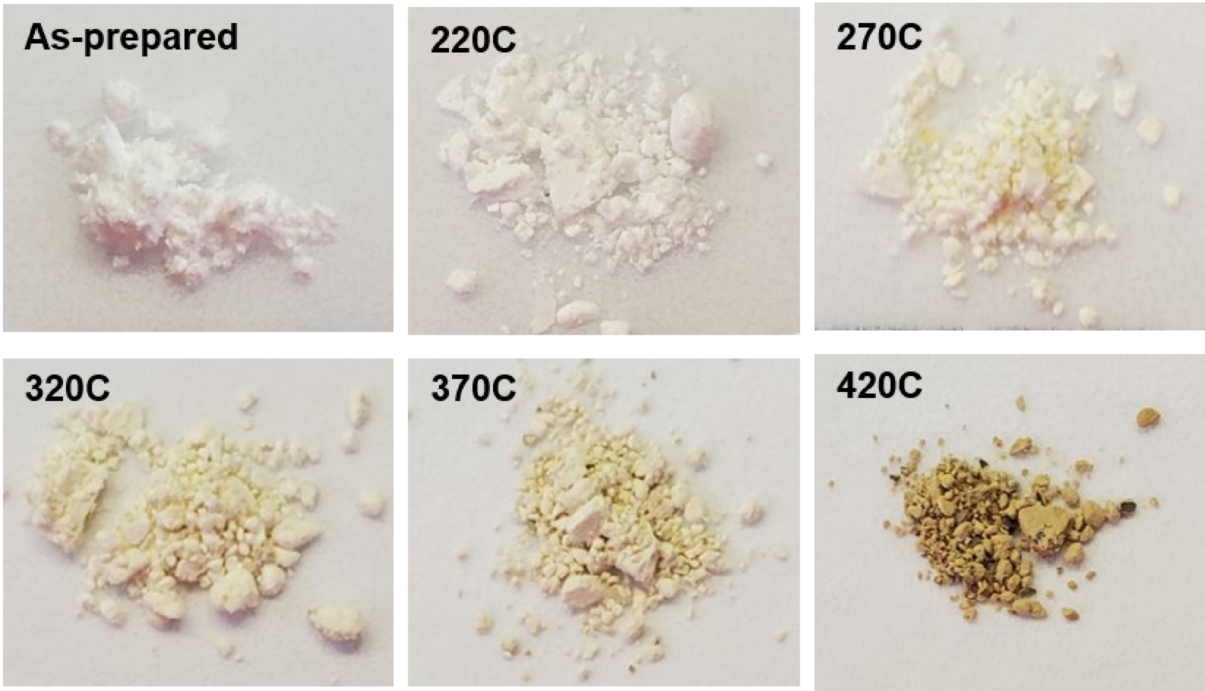

Figure S7. Photograph of CdIF-1 and a_TCdIF-1 samples with different heating temperatures. All samples were immediately cooled naturally without soaking time.

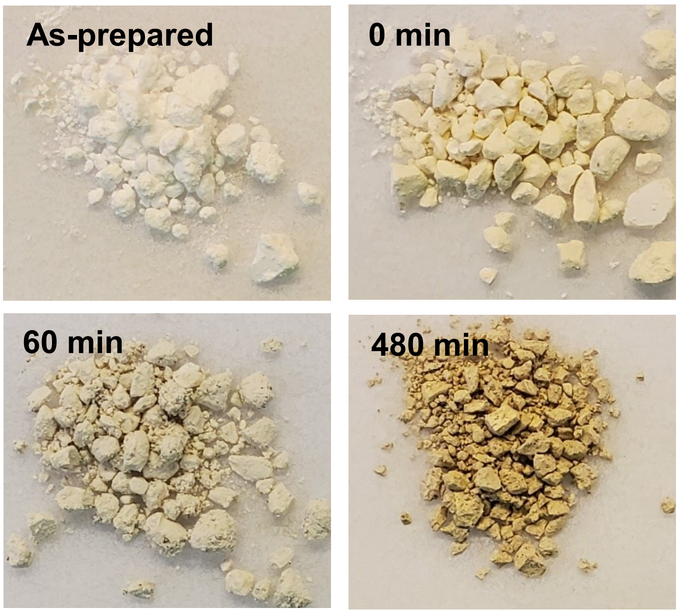

Figure S8. Photograph of CdIF-1 and a_TCdIF-1 samples with different soaking time at 320 ^{o}C.

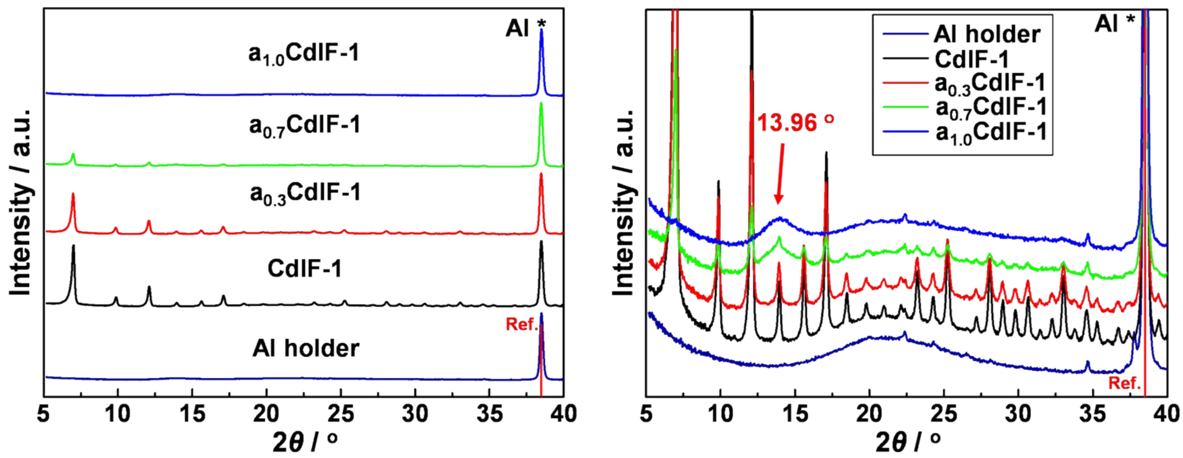

Figure S9. XRD patterns of CdIF-1 and a_TCdIF-1. The right figure is the rearranged image of the left figure. The reference peak was taken by aluminum syn. 00-004-0787 (JCPDS).

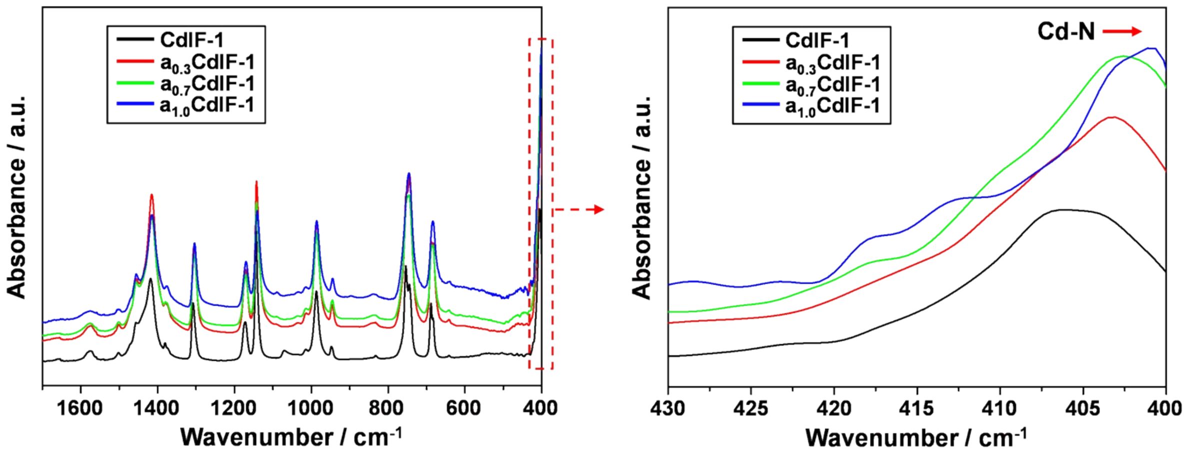

Figure S10. FT-IR spectra of CdIF-1 and a_TCdIF-1.

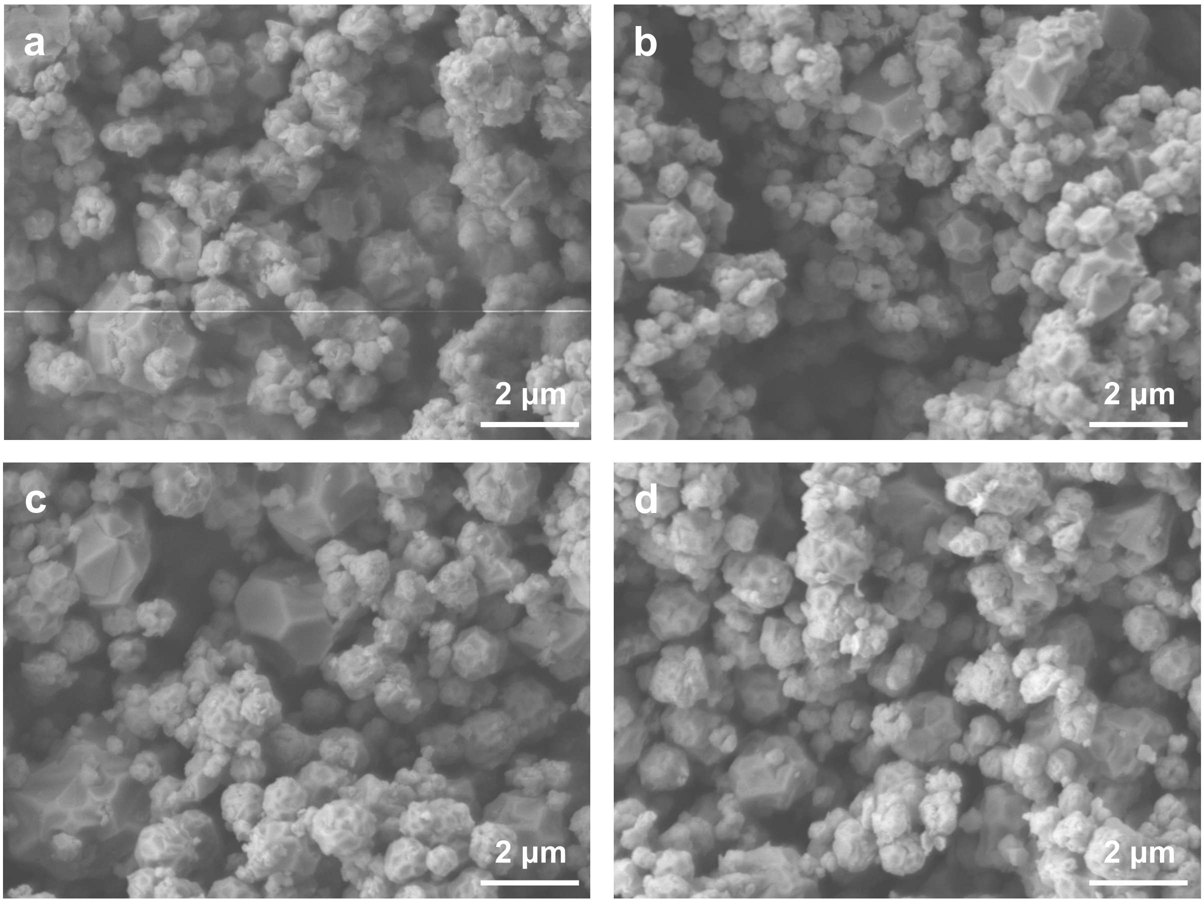

Figure S11. SEM images of (a) CdIF-1, (b) $a_{0.3}$CdIF-1, (c) $a_{0.7}$CdIF-1, and (d) $a_{1.0}$CdIF-1.

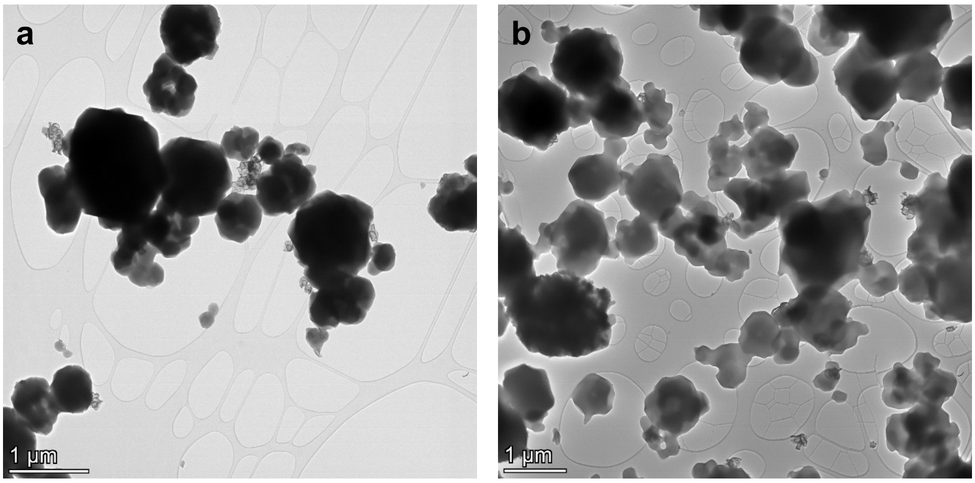

Figure S12. TEM images of (a) CdIF-1 and (b) $a_{1.0}$CdIF-1 at low magnifications.

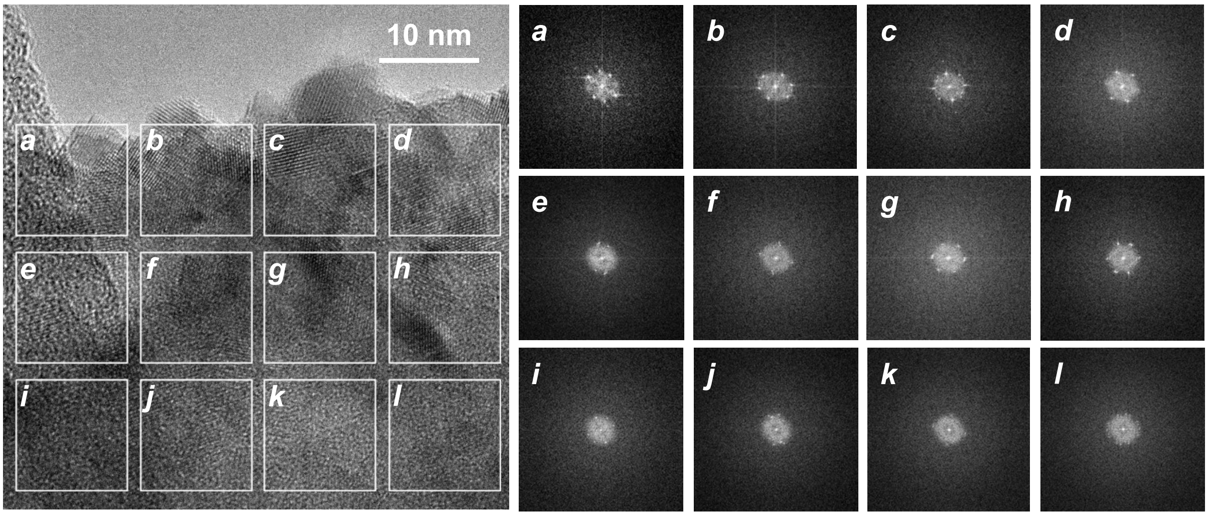

Figure S13. HRTEM image of $a_{0.3}$CdIF-1 and the corresponding FFT diffractions at different positions.

Table S1. BET surface area and pore volume determined by N_2 physisorption at 77 K

	CdIF-1	**$a_{0.3}$CdIF-1**	**$a_{0.7}$CdIF-1**	**$a_{1.0}$CdIF-1**
BET surface area / $cm^2\ g^{-1}$	1412.7	~ 400	91.7	16.9
Pore volume / $cm^3\ g^{-1}$	0.66	~ 0.1	0.04	0.007

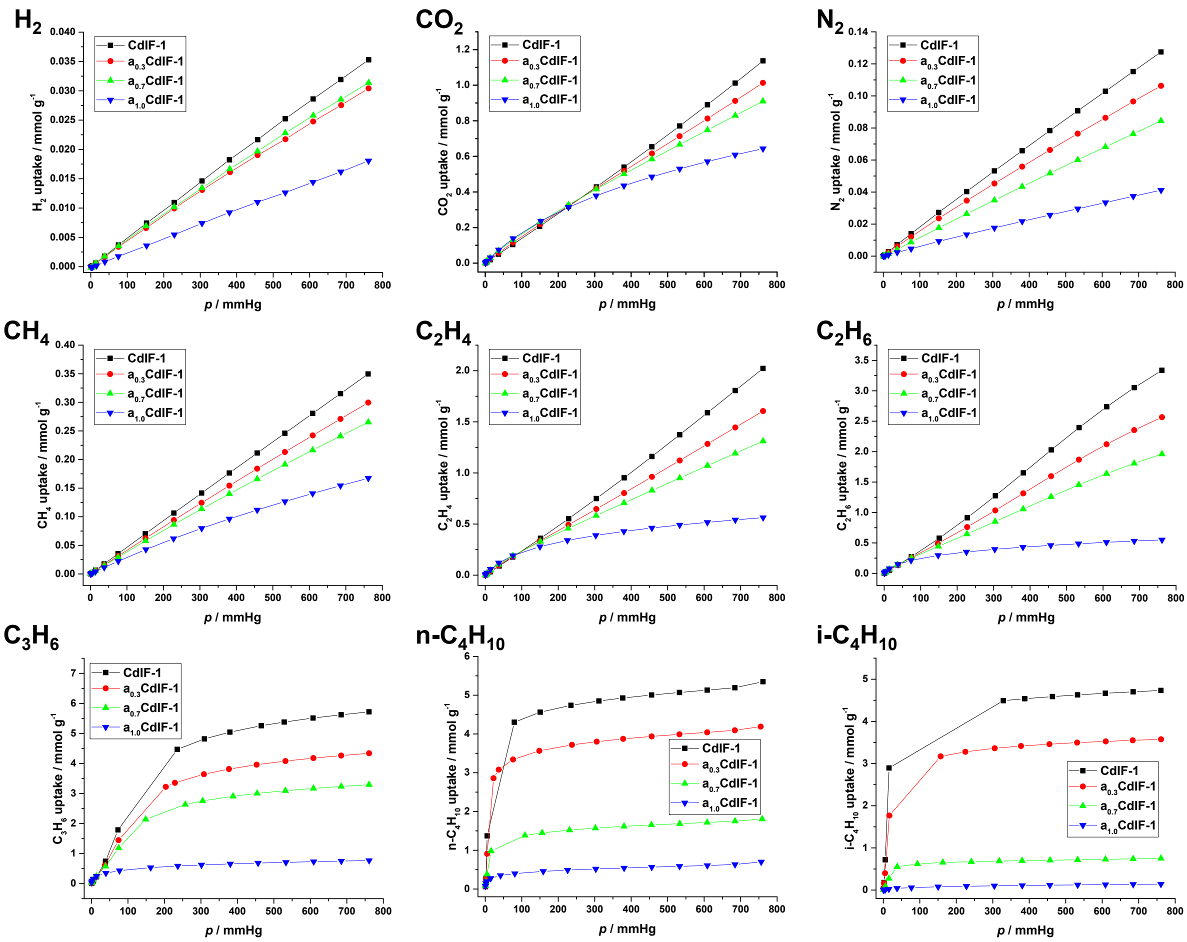

Figure S14. Adsorption isotherms of various gas molecules for CdIF-1 and a_TCIF-1 at 273 K.

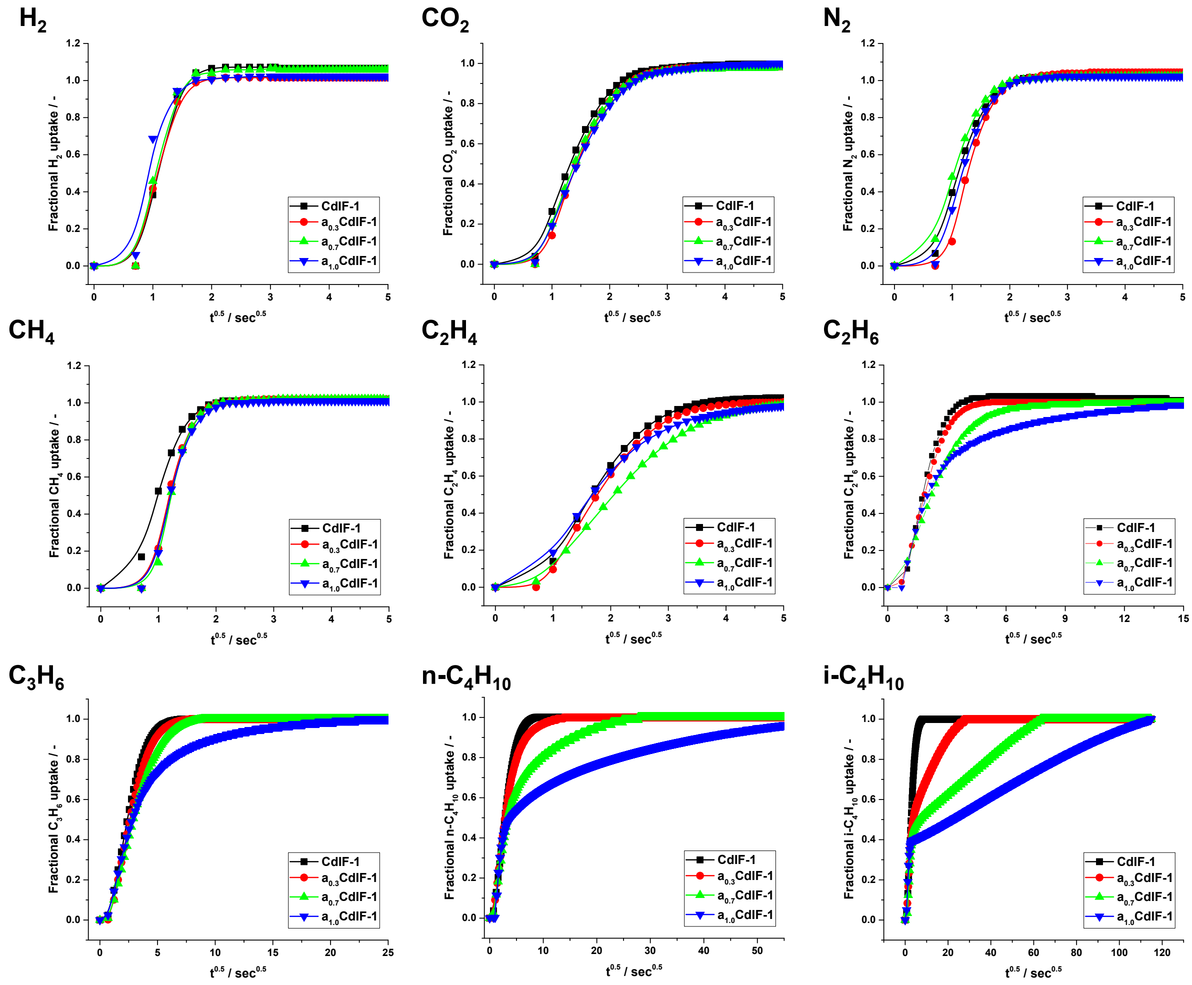

Figure S15. Kinetic uptakes of various gas molecules for CdIF-1 and a_TCIF-1 at 273 K.

Table S2. Langmuir fitting parameters

Sample	Gas	273 K		298 K		323 K	
		C_s / mmol g^{-1}	**b / mmHg^{-1}**	**C_s / mmol g^{-1}**	**b / mmHg^{-1}**	**C_s / mmol g^{-1}**	**b / mmHg^{-1}**
CdIF-1	C_3H_6	7.42	0.005	8.65	0.002	n/a	n/a
	C_3H_8	6.06	0.009	6.14	0.004	n/a	n/a
	n-C_4H_{10}	5.24	0.055	4.83	0.025	4.64	0.009
	i-C_4H_{10}	4.79	0.061	4.58	0.019	4.52	0.007
$a_{0.3}$CdIF-1	C_3H_6	5.44	0.006	6.28	0.002	n/a	n/a
	C_3H_8	4.56	0.009	4.70	0.003	n/a	n/a
	n-C_4H_{10}	4.08	0.072	3.74	0.026	3.28	0.010
	i-C_4H_{10}	3.64	0.045	3.57	0.019	3.28	0.006
$a_{0.7}$CdIF-1	C_3H_6	4.04	0.006	4.48	0.002	2.55	0.001
	C_3H_8	3.40	0.010	3.45	0.003	1.96	0.001
	n-C_4H_{10}	1.71	0.065	1.54	0.025	1.27	0.010
	i-C_4H_{10}	0.76	0.043	1.00	0.013	0.35	0.004
$a_{1.0}$CdIF-1	C_2H_4	0.71	0.004	0.56	0.002	0.55	0.001
	C_2H_6	0.64	0.006	0.50	0.003	0.43	0.002
	C_3H_6	0.76	0.021	0.60	0.009	0.51	0.004
	C_3H_8	0.61	0.023	0.49	0.011	0.38	0.005
	n-C_4H_{10}	0.60	0.045	0.47	0.026	0.33	0.007
	i-C_4H_{10}	0.16	0.007	0.24	0.012	0.19	0.004

Table S3. Corrected diffusivities (D_o) at 273K

Unit: $cm^2\ sec^{-1}$	**CdIF-1**	**$a_{0.3}$CdIF-1**	**$a_{0.7}$CdIF-1**	**$a_{1.0}$CdIF-1**
H_2	$2.19 \times 10^{-9} \pm 1.66 \times 10^{-10}$	$2.54 \times 10^{-9} \pm 3.89 \times 10^{-10}$	$1.21 \times 10^{-9} \pm 5.88 \times 10^{-10}$	$1.40 \times 10^{-9} \pm 8.46 \times 10^{-10}$
N_2	$2.80 \times 10^{-10} \pm 3.74 \times 10^{-11}$	$2.70 \times 10^{-10} \pm 4.09 \times 10^{-11}$	$1.53 \times 10^{-10} \pm 6.64 \times 10^{-11}$	$2.74 \times 10^{-10} \pm 1.33 \times 10^{-11}$
CH_4	$5.98 \times 10^{-10} \pm 7.04 \times 10^{-11}$	$5.61 \times 10^{-10} \pm 1.51 \times 10^{-11}$	$3.42 \times 10^{-10} \pm 1.48 \times 10^{-10}$	$6.62 \times 10^{-10} \pm 1.83 \times 10^{-10}$
CO_2	$7.93 \times 10^{-10} \pm 2.38 \times 10^{-11}$	$7.37 \times 10^{-10} \pm 8.80 \times 10^{-11}$	$4.61 \times 10^{-10} \pm 1.99 \times 10^{-10}$	$8.31 \times 10^{-10} \pm 1.48 \times 10^{-10}$
C_2H_4	$3.55 \times 10^{-10} \pm 3.61 \times 10^{-11}$	$3.34 \times 10^{-10} \pm 4.15 \times 10^{-11}$	$2.20 \times 10^{-10} \pm 4.57 \times 10^{-11}$	$2.50 \times 10^{-10} \pm 6.37 \times 10^{-11}$
C_2H_6	$3.27 \times 10^{-10} \pm 7.31 \times 10^{-11}$	$2.36 \times 10^{-10} \pm 5.44 \times 10^{-11}$	$1.54 \times 10^{-10} \pm 5.15 \times 10^{-11}$	$1.58 \times 10^{-10} \pm 9.39 \times 10^{-11}$
C_3H_6	$1.35 \times 10^{-10} \pm 2.14 \times 10^{-11}$	$1.06 \times 10^{-10} \pm 4.59 \times 10^{-12}$	$7.49 \times 10^{-11} \pm 2.49 \times 10^{-11}$	$6.06 \times 10^{-11} \pm 1.80 \times 10^{-11}$
C_3H_8	$1.21 \times 10^{-10} \pm 1.45 \times 10^{-11}$	$7.05 \times 10^{-11} \pm 1.74 \times 10^{-11}$	$2.42 \times 10^{-11} \pm 9.94 \times 10^{-12}$	$3.11 \times 10^{-12} \pm 1.19 \times 10^{-12}$
n-C_4H_{10}	$8.09 \times 10^{-11} \pm 2.44 \times 10^{-12}$	$5.55 \times 10^{-11} \pm 8.36 \times 10^{-12}$	$1.11 \times 10^{-11} \pm 6.89 \times 10^{-12}$	$1.17 \times 10^{-12} \pm 5.36 \times 10^{-13}$
i-C_4H_{10}	$5.38 \times 10^{-11} \pm 2.03 \times 10^{-11}$	$6.55 \times 10^{-12} \pm 1.24 \times 10^{-12}$	$2.74 \times 10^{-13} \pm 9.94 \times 10^{-14}$	$7.66 \times 10^{-14} \pm 1.71 \times 10^{-14}$

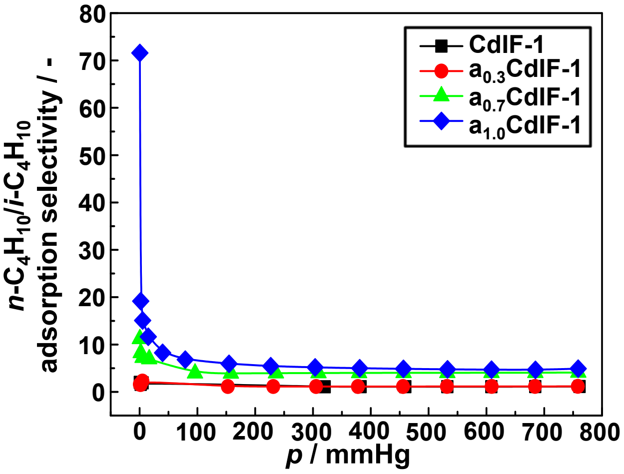

Figure S16. Ideal n-C_4H_{10}/i-C_4H_{10} adsorption selectivity of CdIF-1 and a_TCdIF-1.

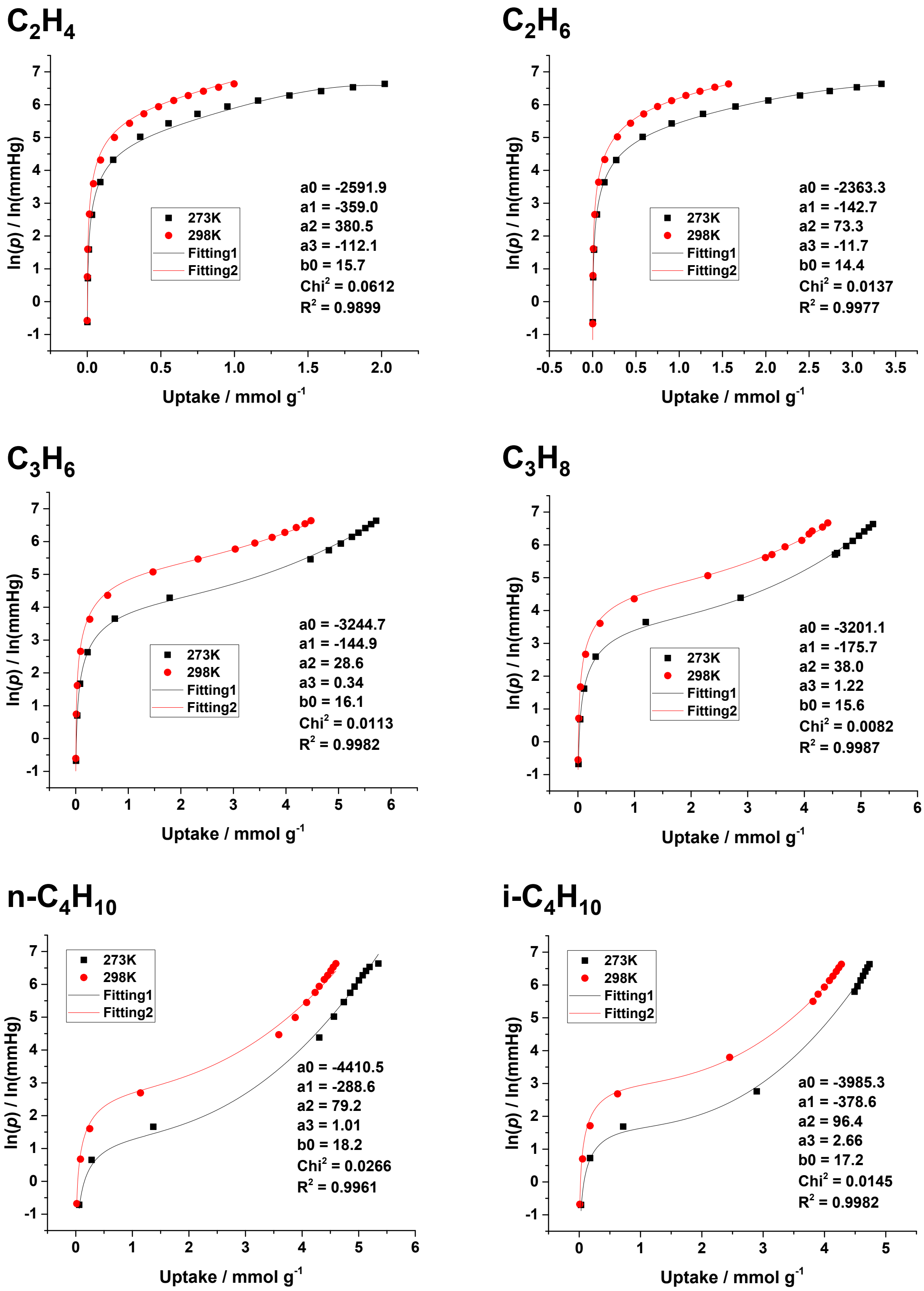

Figure S17. Virial fitting of adsorption isotherms for CdIF-1.

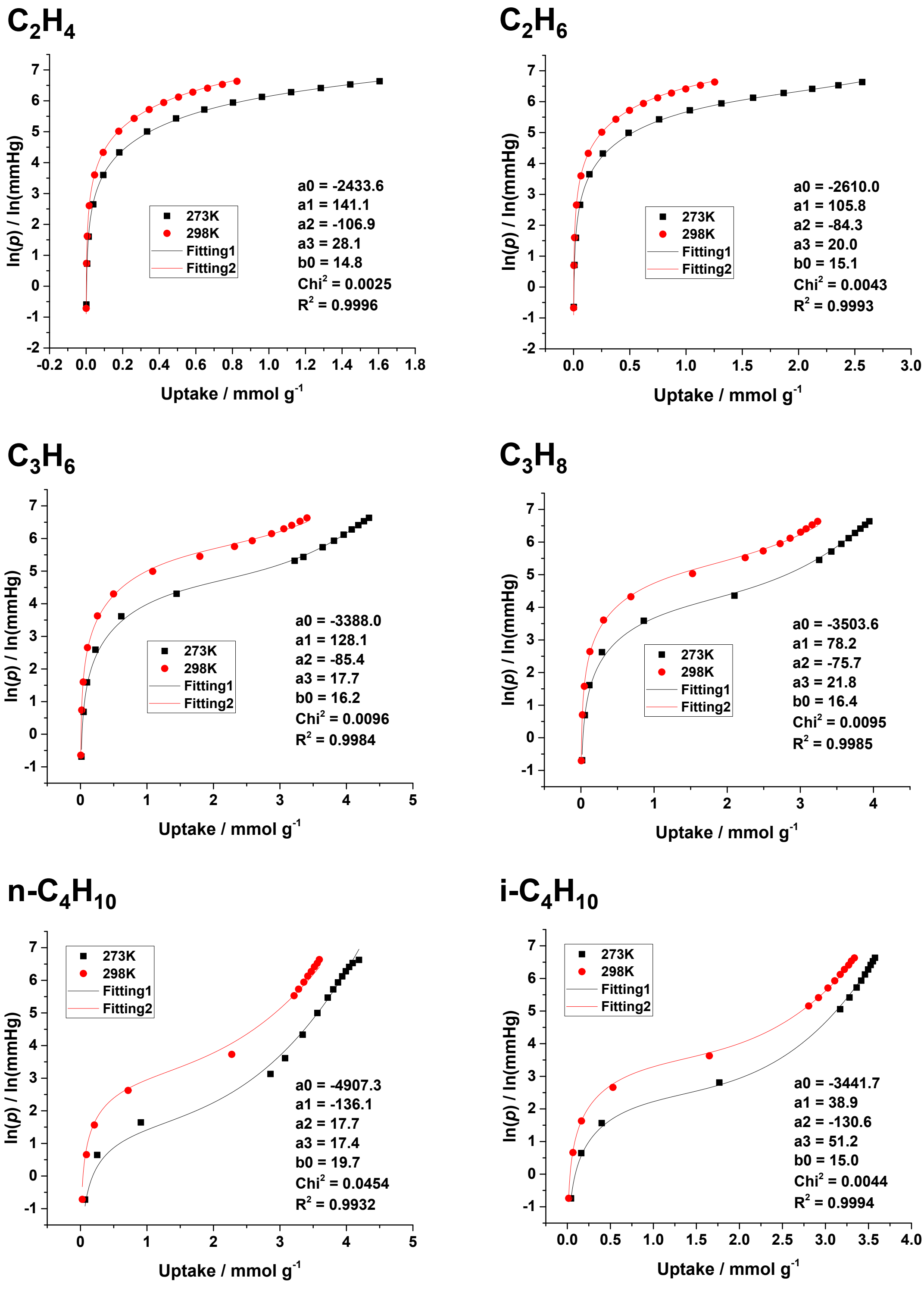

Figure S18. Virial fitting of adsorption isotherms for $a_{0.3}$CdIF-1.

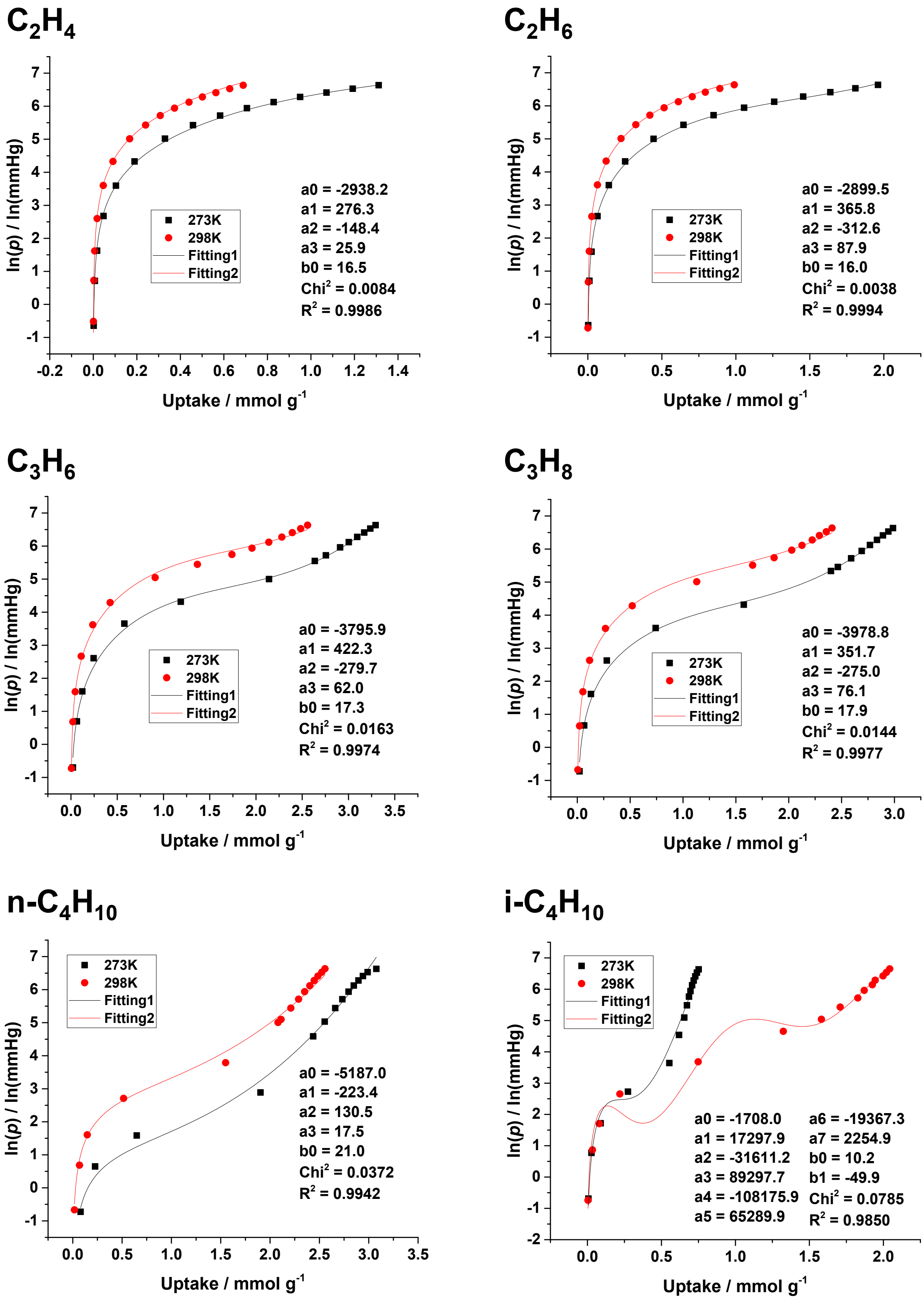

Figure S19. Virial fitting of adsorption isotherms for $a_{0.7}$CdIF-1.

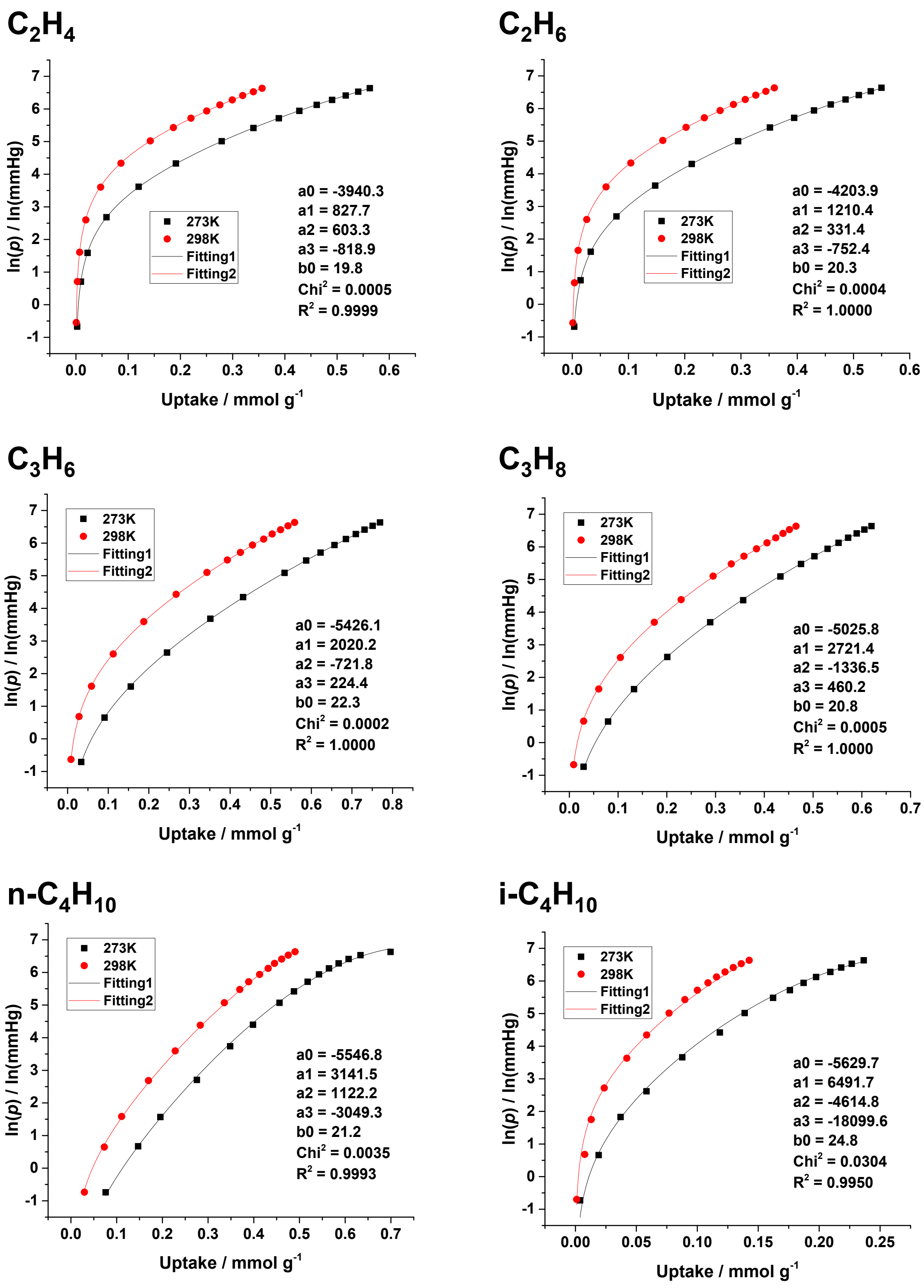

Figure S20. Virial fitting of adsorption isotherms for $a_{1.0}$CdIF-1.

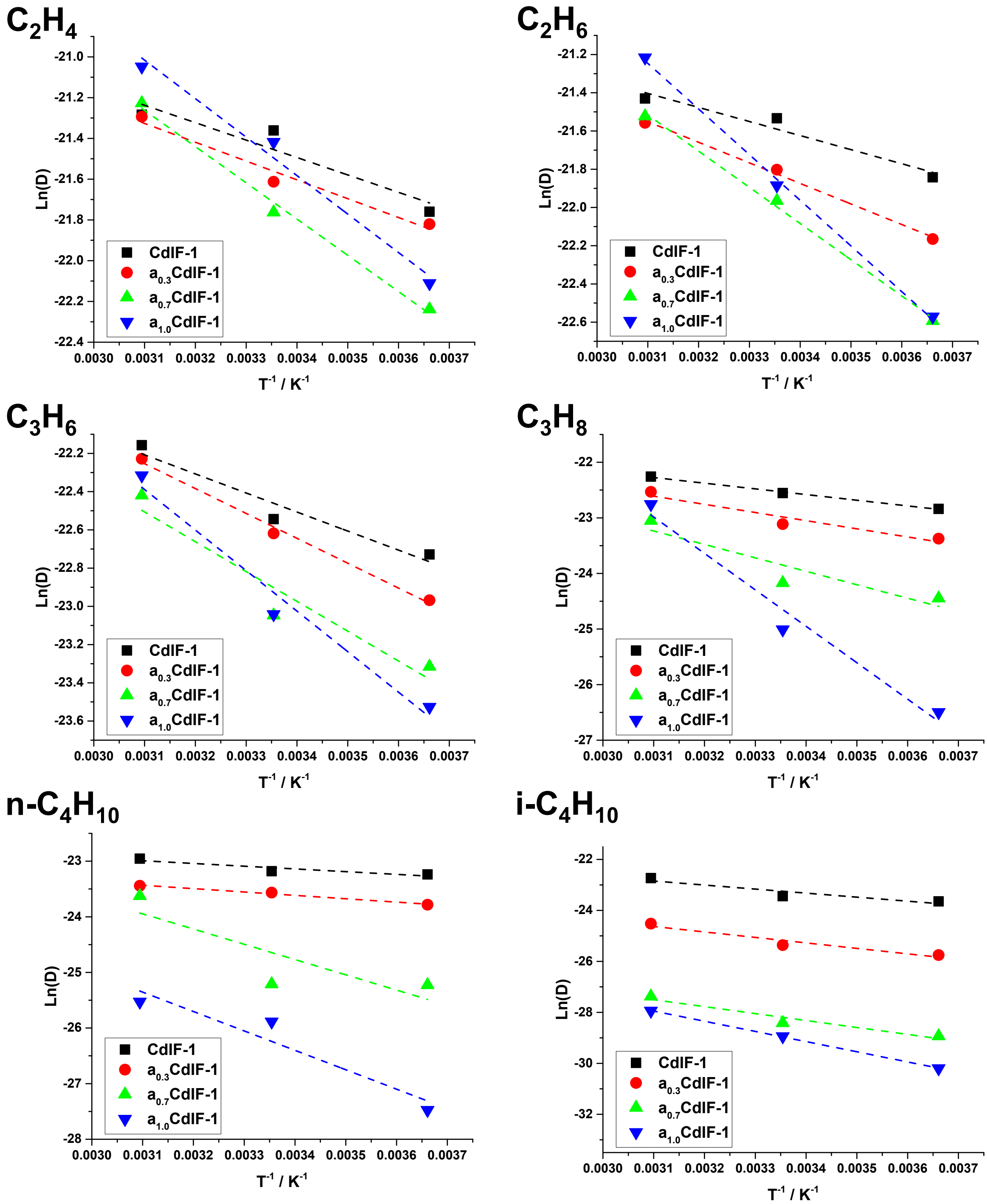

Figure S21. Arrhenius plots for the activation energy of diffusion (E_a).

Table S4. Isosteric enthalpy of adsorption (ΔH^{o}_{ads})

Unit: kJ mol^{-1}	**CdIF-1**	**a$_{0.3}$CdIF-1**	**a$_{0.7}$CdIF-1**	**a$_{1.0}$CdIF-1**
C_2H_4	21.5 ± 2.7	20.2 ± 0.5	24.4 ± 1.0	32.8 ± 0.3
C_2H_6	19.6 ± 1.3	21.7 ± 0.7	24.1 ± 0.7	35.0 ± 0.1
C_3H_6	27.0 ± 1.3	28.2 ± 1.2	31.6 ± 1.5	45.1 ± 0.2
C_3H_8	26.6 ± 1.1	29.1 ± 1.2	33.1 ± 1.4	41.8 ± 0.3
n-C_4H_{10}	36.7 ± 2.2	40.8 ± 2.6	43.1 ± 2.5	46.1 ± 0.7
i-C_4H_{10}	33.1 ± 1.8	28.6 ± 0.9	14.2 ± 6.1	46.8 ± 2.0

Table S5. Activation energy of diffusion (E_a)

Unit: kJ mol^{-1}	**CdIF-1**	**a$_{0.3}$CdIF-1**	**a$_{0.7}$CdIF-1**	**a$_{1.0}$CdIF-1**
C_2H_4	7.10 ± 2.38	7.68 ± 1.31	14.78 ± 1.22	15.70 ± 1.98
C_2H_6	6.12 ± 1.45	8.94 ± 0.56	15.75 ± 0.82	19.85 ± 0.81
C_3H_6	8.29 ± 2.11	10.82 ± 0.87	12.97 ± 3.67	17.63 ± 2.89
C_3H_8	8.49 ± 0.49	12.20 ± 3.27	20.10 ± 8.12	54.49 ± 9.12
n-C_4H_{10}	10.08 ± 1.63	15.04 ± 0.55	22.81 ± 14.41	29.02 ± 9.04
i-C_4H_{10}	12.54 ± 4.93	17.87 ± 4.70	24.12 ± 5.55	33.20 ± 0.56